Calculated Properties of the Active Site Complex of Oxidized Rubredoxins

I. Electron Distribution and Electronic Energies as a Function of Conformation

Gilda Harris Loew, Michael Chadwick, and David A. Steinberg

Department of Genetics, Stanford University Medical Center, Stanford, California 94305

In rubredoxins, the simplest class of iron-sulfur, electron-transport proteins, the center of biological activity is a single Fe atom which is surrounded by a distorted tetrahedral array of four cysteine sulfur atoms. In addition to its electron-transport characteristics, a number of physical properties of these proteins have been determined, all of which depend crucially on the conformation and electron distribution and energy of the active site complex. Thus, in this initial study, using a semi-empirical MO program called Iterative Extended Hückel Theory (IEHT), we have calculated the variation in electron distribution and energies of the Fe–S active site complex as a function of its conformation. Ten conformers were chosen which span a symmetry range from that determined by X-Ray crystal structure analysis to an idealized regular tetrahedral symmetry. The differences in electron distribution and electronic energies obtained for these 10 conformers are reflected in all observable properties of the protein calculation of these properties, using the results reported here, are the subject of our subsequent papers in this series.

Key words: Electronic structure of oxidized rubredoxins – Rubredoxin (oxidized) – Iron-sulfur proteins

1. Introduction and Background

The simplest class of iron-sulfur (non-heme) proteins that participate in numerous biological electron-transport reactions are the rubredoxins, containing one Fe atom and 4 cysteine residues per protein molecule, with no labile sulfur present. Rubredoxins undergo reversible one-electron oxidation reduction with a typical E_0 value of -0.05 V [1] and both forms are stable. An X-ray diffraction study of the oxidized rubredoxin from Clostridium Pasteurianum has been made to a resolution of 1.5 Å [2] and reveals that the Fe atom is surrounded by the four sulfur atoms of the cysteine residues in a distorted tetrahedral array. The X-ray structure is shown in Fig. 1 [2]. Among other properties of both the oxidized and reduced forms of rubredoxins which have been measured are: the optical [1, 3, 4], electron spin resonance [6] and Mossbauer resonance [5, 7] spectra as well as magnetic moment [5].

All of these properties depend crucially on the electron distribution, energy and conformation at the active site and are often thought of as "probes" of these characteristics. Yet no one-to-one correspondence exists between values of these properties and the possible conformations and electron distributions of the active
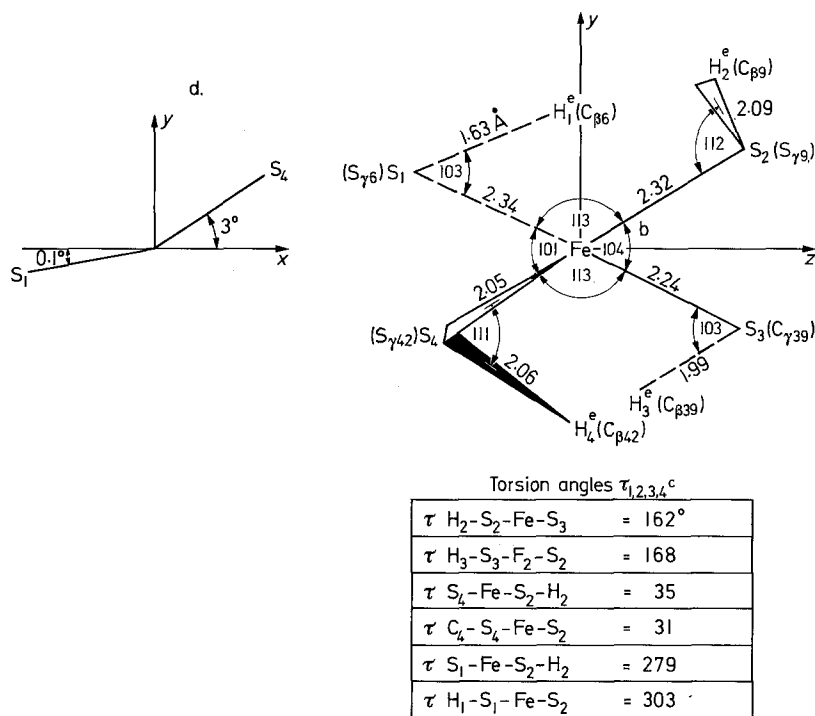
Fig. 1. X-ray structure of active site complex (a) Ref. [2b] in text. (b) Angles not shown: S_1–Fe–$S_3 = 108°$, S_2–Fe–$S_4 = 115°$. (c) Torsion angles involving H atoms. τ_{1234} = rotation of atom 4 into 1; counterclockwise around $3 - 2$. (d) S_1–Fe–S_4 slightly displaced from xz plane as indicated; S_2–Fe–S_3 in yz plane. (e) In conformer O_1 H are placed in position of BC atoms. In conformer O_2 all S_i–H_i bonds are shortened to $1.34°$

site. Up to now the experimental results are simply consistent with the notion of a high-spin ferric complex for the oxidized state and a high-spin ferrous complex for the reduced state, with the local symmetry about the Fe atom having some kind of "rhombic character", i.e. less than axial symmetry. Thus, we felt that their value as "probes" would be greatly increased if the behavior of these properties were calculated as a function of specific conformational variations, a calculation which has not heretofor been done.

The model for the active site complex chosen for this study includes the Fe atom, the 4 cysteine S atoms and the replacement of the βC atoms bound to the S by H atoms. This latter simplification greatly reduced the amount of computation time needed and preliminary calculations with CH_3 groups on the S atoms instead of the H atoms revealed that differences between them were not significant for the properties we were interested in calculating. All the valence orbitals and electrons of each atom were included in the molecular orbital calculations made. For the oxidized system there are a total of 39 atomic orbitals: nine for Fe ($4s$, $4p$, and $3d$), 4 for each S ($3s$, $3p$) and 1 for each H ($1s$). The complex which is formally $[Fe^{+3} + 4SH^-]$ has 37 valence electrons and a net negative charge, presumably balanced by a nearby cation.

To obtain a description of the electron distribution and electronic energies for 10 different geometric variation of the active site complex, we have used a working computer program, based on a semi-empirical molecular orbital method called Iterative Extended Hückel Theory (IEHT), essentially in the form developed by Zerner and Gouterman for their study of iron heme complexes [8, 9]. The results of such calculations give configuration energies and reasonable electron distributions in the molecule for each geometry chosen. From these, all of the observed properties mentioned above can be calculated in some approximation.

2. Description of the Set of Conformers Studied

Among the 10 specific conformers of the active site complex of oxidized rubredoxins we have chosen to study the totally experimentally determined conformation shown in Fig. 1 [2b] with H atoms in the place of βC atoms (conformer O_1). The main features of this X-ray-diffraction-determined structure of the Fe–S complex are that none of the Fe–S bond lengths or S–Fe–S bond angles are equal and that one bond length is appreciably shorter than the rest. The net result is that the array of S atoms about the Fe atom in the protein is too distorted to belong to any symmetry point group. One variation made was to shorten all the S–H bond lengths to 1.34 Å, while leaving the remainder of the X-ray determined structure the same (conformer O_2).

The eight remaining geometric variations we have considered are various idealizations of the crystal structure, increasing the symmetry up to a totally regular tetrahedral array of S and H ligands. These eight variations are shown in Fig. 2.

In conformers A, B and C we force the 4S atoms to be in two perpendicular planes yz and xz. Such a change corresponds to a significant change in only the S_1–Fe–S_3 bond angle from 108–113.6°. In conformers A and B, Fe–S bond lengths determined from an earlier refinement of crystal data are used, and the position of the H atoms is varied, corresponding to a small change in position of the cysteine residues. Conformer A has a "pinwheel" arrangement of H atoms, while in conformer B the H atoms are arranged to have C_{2v} symmetry with the z axis as the two-fold rotation axis. Neither conformer belongs to any point group. Conformer C has two sets of equivalent S atoms, with two different Fe–S bond lengths; and the H atoms are as in conformer B. Thus, there is no unique short bond and the entire active site complex has C_{2v} symmetry.

In conformers F and G, the short bond is preserved as a three-fold axis rotation (z-axis) and the other three S atoms made equivalent with Fe–S bond lengths of 2.35 Å. Conformers F and G differ only in the placement of the H atoms. Both have one co-linear Fe–S–H bond along the z axis. In conformer F the remaining three H atoms bound to the equivalent S atoms are made coplanar with them giving the molecule overall C_3 symmetry, while in conformer G, these S atoms all have their H atoms "cis" to the three-fold axis, thus giving the molecule C_{3v} symmetry.

In conformer D and E all 4 sulfur atom ligands are equivalent and are in a regular tetrahedral array with an Fe–S bond length of 2.00 Å. In conformer D the H atoms are arranged so as to preserve three two-fold axes (x, y, z) thus giving the molecule overall D_2 symmetry. Conformer E is strictly T_D with the S ligand
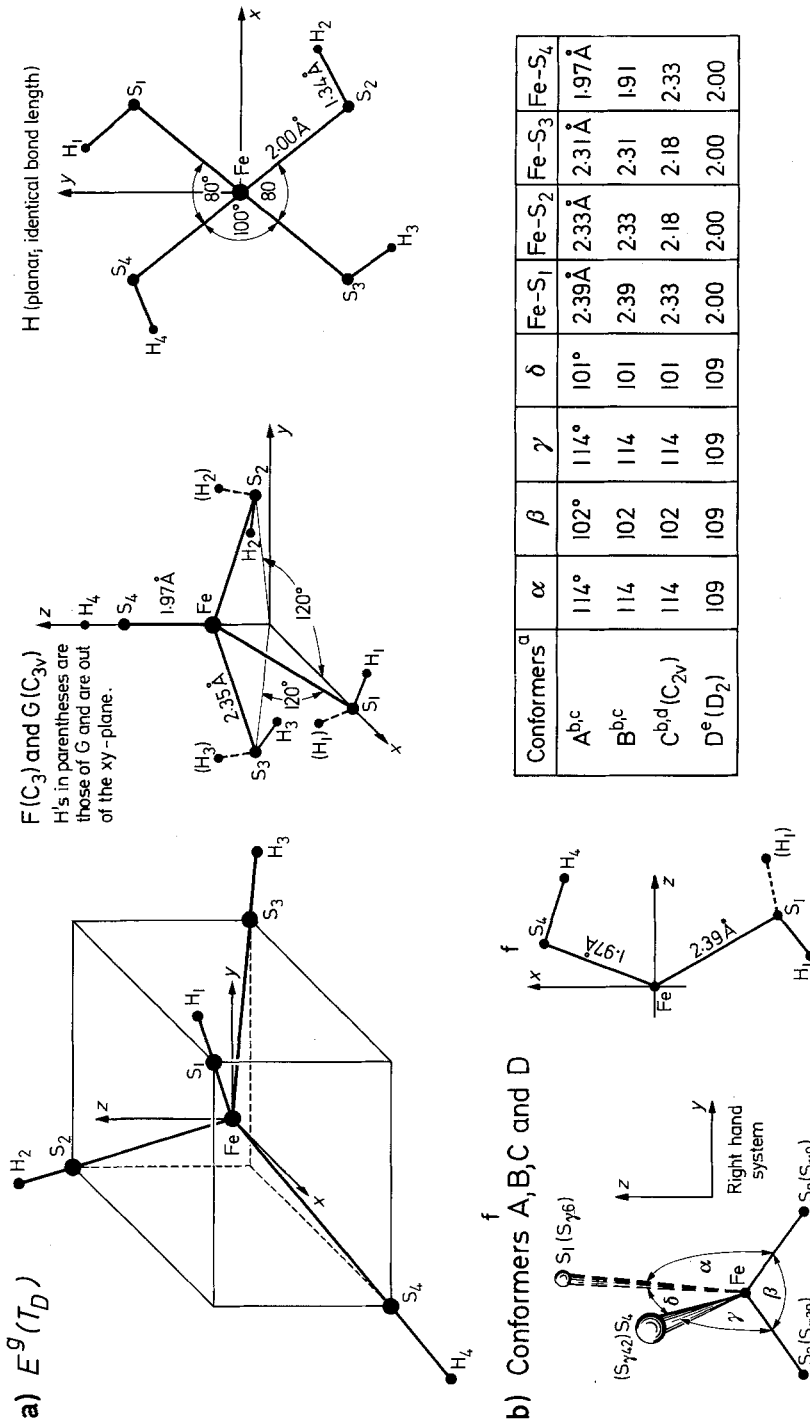
a) $E^g(T_D)$

F(C_3) and G(C_{3v})

H's in parentheses are those of G and are out of the xy–plane.

H (planar; identical bond length)

b) Conformers A,B,C and D

Right hand system

Conformers[a]	α	β	γ	δ	Fe-S₁	Fe-S₂	Fe-S₃	Fe-S₄
A[b,c]	114°	102°	114°	101°	2.39Å	2.33Å	2.31Å	1.97Å
B[b,c]	114	102	114	101	2.39	2.33	2.31	1.91
C[b,d](C_{2v})	114	102	114	101	2.33	2.18	2.18	2.33
D[e](D_2)	109	109	109	109	2.00	2.00	2.00	2.00

Fig. 2. Eight conformational variations of active site complex.(a) In A, B, C, D S_2, S_3 are in yz and $S_1 S_4$ in xz plane, and all $S–H$ distances are 1.34 Å. (b) Slight alteration ($\leqq 2°$) in experimental values of α, β, γ, δ for A, B, C and changing S₁-Fe-S₃ from 108° to 113.6° are required to fulfill this conditions. (c) Values of Fe–S[i] in A and B are from Jensen X-ray data of March 1972; while those in O^1 and O^2 are from data of October 1972 (both private communication).(d) Conformer C is a C_{2v} idealization of B with S_1, S_4 and S_2, S_3 pairwise equivalent.(e) Conformer D is a still further idealization with all four S atoms equivalent and arranged in a regular tetrahedral array.(f) In conformer A, H^1 represented by solid line and in B dotted line. The H's in the yz plane are similarly arranged; in a pinwheel fashion in A and a mirror image in B. Conformer C is a C_{2v} idealization of B, while the H atoms in D have a pinwheel arrangement.(g) Conformer E is totally tetrahedral with the same tetrahedral skeleton for the S's as D but rotated by 45° around the z axis and with all Fe–S–H bonds linear

skeleton rotated by 45° around the z axis from conformer D and the H atoms made co-linear with the Fe–S bonds. We have also included a totally planar (xy) arrangement of the Fe, S and H atoms with C_2 symmetry. Conformers D, E and H are unrealistic candidates for the actual active site conformation in rubredoxins and they were included mainly for didactic reasons. In these extreme conformations the values of Fe–S bond lengths chosen are very secondary to the effect of symmetry on the observed properties.

Thus, the 10 conformers considered span a symmetry range from completely tetrahedral to the no-symmetry crystal structure determined from X-ray analysis. The question now is, how sensitive is the electron distribution and energy of the active site to these symmetry changes?

3. Nature and Energy of the 5 Fe-d-Ligand Antibonding Orbitals as a Function of Conformation

The coordinates of each of the 10 geometric conformers of the active site complex just described were used as input to a working program based on the Iterative Extended Hückel Theory (IEHT), well described in the literature [8, 9]. The result is a set of molecular orbitals, obtained as linear combinations of interacting atomic orbitals: $\Phi_i = \sum_j^{a.o.} c_{ij} X_j$ and a corresponding set of orbital energies (ε_j) which are eigenfunctions and eigenvalues of the one-electron Hamiltonian respectively, as well as eigenfunctions of the symmetry operations of the point group of the molecule. The portion of molecular energy calculated by the IEHT method is the valence configuration energy, i.e. the sum of the energies of the occupied orbitals of a specified configuration with some electron correlation introduced in the charge iteration process.

For the active site complex, the configuration that corresponds to the sextet state which is known to be the ground state of the Fe in the protein is one with 5 half-filled molecular orbitals: $(1)^2 (2)^2 \dots (16)^2 (17)(18)(19)(20)(21)$. The electron distribution in this configuration was obtained for all 10 geometric isomers. The

Table 1. Net atomic charges in active site complex[a]

Atom	Conformation									
	O_1	O_2	A	B	C	D	E	F	G	H
Fe	+0.12	+0.06	+0.05	+0.05	+0.06	+0.05	+0.03	+0.04	+0.04	0
S_1	−0.15	−0.24	−0.24	−0.24	−0.23	−0.21	−0.21	−0.24	−0.24	−0.21
S_2	−0.13	−0.23	−0.23	−0.24	−0.23	−0.21	−0.21	−0.24	−0.24	−0.235
S_3	−0.12	−0.23	−0.22	−0.23	−0.22	−0.21	−0.21	−0.24	−0.24	−0.235
S_4	−0.09	−0.20	−0.18	−0.18	−0.22	−0.21	−0.21	−0.18	−0.17	−0.21
H_1	−0.07	−0.04	−0.04	−0.04	−0.04	−0.05	−0.04	−0.046	−0.05	−0.01
H_2	−0.20	−0.04	−0.05	−0.04	−0.04	−0.05	−0.04	−0.046	−0.05	−0.04
H_3	−0.17	−0.04	−0.04	−0.04	−0.03	−0.05	−0.04	−0.046	−0.05	−0.04
H_4	−0.17	−0.04	−0.03	−0.03	−0.03	−0.05	−0.04	−0.01	0	−0.01

[a] Fractional electron charge.

net charge on all atoms obtained from a Mulliken population analysis [10] of the filled mos is given in Table 1. We see from this table that the Fe atom has only a small positive charge. Variations in the negative charges on the S and H ligands reflect their geometric inequivalence. As is usual, even with a net (–) charge on the complex, there is no large charge buildup on any atom in the complex.

The half-filled molecular orbitals 17–21 are primarily Fe d orbitals with some bonding to the S ligands. Assigning 5 electrons to these orbitals corresponds to a formal ferric ion d^5 configuration. The dramatic way in which both the nature and relative energies of these crucial "ligand field orbitals" depend on symmetry is shown in Fig. 3. It should be kept in mind that the 10 variations studied involve a chemically identical Fe–SH complex. For each MO, the fraction of electrons in the principal d orbitals obtained from a Mulliken population analysis [10] is given together with the calculated molecular orbital energies.

These characteristics reflect the way each Fe d orbital interacts with the appropriate symmetry-combination of sulfur p orbitals in each conformer. In conformers O_1 and O_2 with the total crystal structure geometry of the complex, there is no orbital degeneracy and the lowest lying ligand field orbital is 77% d_z^2 while the highest energy orbital is 51% $d_{x^2-y^2}$. The three "t_2" orbitals mix with each other and lie in energy between the two e orbitals. The nature and energy ordering of the 5 molecular orbitals is unchanged when the S–H bond is shortened to 1.34 Å (O_2). Clearly, while the crystal structure symmetry is often described as a "distorted tetrahedron" the molecule has no symmetry and the nature and energy ordering of the ligand field molecular orbitals have no direct correlation with those in T_d symmetry.

In conformers A and B, which also have no symmetry, changing the position of the H atoms but keeping the S atoms essentially in their experimentally determined positions does not significantly alter the nature of the energy-ordered ligand fields mos.

A more significant alteration of the crystal structure results was made in conformer C where the S atoms are pairwise equivalent and the enture molecule has C_{2v} symmetry. As in the O, A and B conformers, the lowest energy orbital is still d_z^2 and the highest $d_{x^2-y^2}$ but both are appreciably more localized. The three "t_2" orbitals do not mix at all in C_{2v} symmetry and again lie between the two split "e" orbitals.

In the planar (xy) conformer (H) with C_2 symmetry, all the ligand field orbitals are split. The lowest lying orbital is 80% d_{xy} and the two highest are nearly degenerate 69% d_{xz}, d_{yz} orbitals; reflecting the symmetry of the placement of the S atoms in the xy plane.

Still another pattern of ligand field orbitals and energy ordering is seen in the two conformers F and G with axial symmetry, i.e. a three-fold axis (z). As shown in Fig. 3, the unique "d_z2" orbital lies between doubly degenerate pairs of orbitals. There are small differences in the behavior of the orbitals in C_3 vs C_{3v} symmetry reflecting the difference in H atom positions.

In conformer E, with totally T_D symmetry, included primarily for didactic reasons, all the Fe d orbitals have approximately the same % d character and the splitting between the doubly degenerate e orbitals which are 63% $d_{x^2-y^2}$ and d_{z^2} and the triple degenerate t_2 orbitals which have 67% d character is only 0.16 eV

Total X tal structure

−8.37	$0.51x^2-y^2$	9.11
−8.67	$0.12xy+20yz+0.20xz$	9.42
0.80 −8.83	$0.41xz+27yz$	9.61
−8.91	$0.47xy+0.13yz$	9.65
−9.17	$0.77z^2$	10.05

A (X-tal + Pinwheel H)

$0.52x^2-y^2$	−8.51
$0.23xy+0.35yz$	−8.61
$0.43xz+0.08x^2-y^2$	−8.83
$0.40xy+0.19yz$	−8.94
$0.86z^2$	−9.16

0.65 eV

B (X-tal + C₂ᵥ H)

$0.53x^2-y^2$	−8.57
$0.23xy+0.34yz$	−8.61
$0.38xz+0.13x^2-y^2$	−8.81
$0.39xy+0.17yz$	−8.93
$0.88z^2$	−9.17

0.60 eV

C (C_{2v})

$0.63x^2-y^2$	−8.61
$0.5yz$ $0.5xz$	−8.80
$0.61xy$	−8.86
$0.97z^2$	−9.26

0.35 eV

D

$0.47x^2-y^2\,0.25(xz+yz)$	−8.15
$0.49z^2+0.16xy$	−8.42
$0.24(yz+xz)$	−8.61
$0.70xy+0.23z^2$	−9.02

0.87 eV

E T_D

$0.34(yz+xz)\,0.67xz\,0.34(yz+xz)$	−8.11
$0.63x^2-y^2$ $0.63z^2$	−8.27

0.16 eV

F (C_3)

$0.30yz+0.16xy$	−8.47
$0.30xz+0.16(x^2-y^2)$	−8.47
$0.58z^2$	−8.64
$0.27yz+0.38xy$	−9.34
$0.27xz+0.38(x^2-y^2)$	−9.34

0.87 eV

G (C_{3v})

$0.26yz+0.22xy$	−8.41
$0.26xz+0.22(x^2-y^2)$	−8.41
$0.69z^2$	−8.79
$0.35xz+0.275x^2-y^2$	−9.15
$0.35yz+0.275xy$	−9.15

0.74 eV

H planar (C_2)

$0.60xz$	−8.11
$0.69yz$	−8.17
$0.71x^2-y^2+14z^2$	−8.51
$0.752z^2+21x^2-y^2+12xy$	−3.67
$0.80xy$	−8.77

0.66 eV

Fig. 3. Nature and energy of the 5 Fe (3d) ligand antibonding orbitals. a Orbital energy in electron volts. b Fraction of electron in principal d orbitals

($1300 \, \mathrm{cm}^{-1}$). In conformers D the Fe–S complex has an identical conformation, with rotation of the x and y axes by $45°$. The change in position of the H atoms lowers the symmetry, but H atomic orbitals have essentially zero electron density in the ligand field molecular orbitals. The observed splitting of the e and t_2 orbitals and the variation in $\% \, d$ character between the two conformers is then a vivid illustration of the effect of molecular symmetry alone on the nature of the bonding of the Fe d orbitals to the same ligands.

The differences in the nature and energy ordering of the 5 half-filled ligand-field molecular orbitals shown in Fig. 3 and just described for the 10 different conformers studied is directly reflected in all of the properties we shall calculate for these conformers: the electric field gradient at the Fe nucleus; the hyperfine interaction of the Fe nuclear spin with the unpaired electron spin; spin-orbit coupling of total states formed from these molecular orbitals; zero field splitting; magnetic moments and g values in electron spin resonance spectra. Each of these properties will be discussed in subsequent work.

For oxidized rubredoxins with a sextet ground state, energy intervals between these d orbitals do not directly correlate to $d - d$ spectral transition energies.

4. Configuration Energies and Term Energies

For each conformer we have calculated the valence configuration energy of eight different "d^5" configurations: the unique sextet configuration; four configurations with three unpaired electrons and three with one unpaired electron as shown in Fig. 5. The relative energies obtained for these eight configurations is also given. We see from this figure that for each symmetry the 5 unpaired electron configurations have the highest energy and the configuration with only mo 19 half-filled has the lowest energy. The energy difference ($^6E_1 - {}^2E_1$) is very symmetry depedent varying from 0.34 eV for T_D to 1.74 eV for C_3 symmetry variation. It is this energy difference which must be overcome if the sextet state is to become the ground state. To achieve this condition, electron correlation energy must be added in some approximation to calculate term energies from configuration energies. Electronic transitions between these states, i.e. all $d - d$ transition are spin forbidden in oxidized rubredoxins and in fact no such transitions are seen. Thus, attempts to evaluate term energies for this purpose would not be fruitful. However, spin orbit coupling among total states also depends on the energy separation between them. And such coupling is a crucial factor in zero-field splitting; g values in electron spin resonance spectra and magnetic moment behavior of the active site complex. For this application then we have attempted the difficult task of estimating energy intervals between the sextet and at least low-lying quartet and doublet states.

Even the most accurate ab initio calculations for transition atoms obtain only 20% of the experimental value of transition energies [11].

Thus, to avoid using term energy differences completely as parameters in calculation of spin-orbit coupling interactions, we have used a semi-empirical method of estimating electron-correlation energy corrections to the configuration energies.

Zerner and Gouterman have already considered the problem of adding electron correlation corrections to the one electron configuration energies

obtained from the IEHT calculations. We have used essentially their formulation [9] as elaborated further in Zerner's thesis [12], but improved it by a calculation of the required two-electron integrals corrections instead of using the experimental values determined from the spectra of Fe atom. The expressions for sextet, quartet and doublet term energies relative to the lowest lying doublet state which we have used are as follows:

$$^6E_1 - {}^2E_1 = \Delta\varepsilon_{62} - 3/5\left[\sum_{i > j = 1}^{5} K_{ij}(\delta_{3d}\text{Fe})\right], \tag{1}$$

$$^4E_i(m_i, n_i, p_i) - {}^2E_1 = \Delta\varepsilon_{4,2} - 2/3(K_{mn} + K_{mp} + K_{np}), \tag{2}$$

$$^2E_i - {}^2E_1 = \Delta\varepsilon_{i1}, \tag{3}$$

where K_{ij} = two election exchange integral = $\left\langle \Phi_i(1)\, \Phi_j(2)\, \dfrac{e^2}{r_{12}}\, \Phi_j(1)\, \Phi_i(2) \right\rangle$

between pairs of half-filled mos (Φ_i) in the configuration which gives rise to the sextet or quartet state.

(m_i, n_i, p_i) are the three half-filled orbitals of the ith quartet configuration. $\Delta\varepsilon$ is the energy difference between the configuration giving rise to the total state in question and the lowest energy doublet configuration, shown in Fig. 4 as $^2E_1$.

These are the same expressions for total state energy used by Zerner and Gouterman. However, they used the experimental values of B and C for Fe atom, 0.1 eV and 0.435 eV [13] in their final numerical estimate of all 10 K_{ij} integrals. We have used the subroutine of an ab initio molecular orbital program called Alchemy [14] to calculate exact values of one and two-centered atomic integrals, and we have written programs which transform the exchange integrals over the complex atomic orbital basis set generated by Alchemy to exchange integrals over the 10 pairs of 5 ligand field molecular orbitals. Separate sets of molecular K_{ij} integrals were obtained for each geometric conformer studied. Using conformer A as a trial case, it was determined that the contribution of the one centered S and two centered Fe–S exchange integrals to K_{ij} was negligible compared to the one centered Fe exchange integral values, and only these were retained. The variation in magnitude of the K_{ij} integrals with orbital exponent and the corresponding variation of the B and C terms is indicated in Table 2. The standard definition of B and C [13] in terms of atomic orbital integrals were used:

$$C \equiv K(2, -1|2, -1); \quad 6B + C = K(2, 1|2, 1)$$

where

$$K(l, m_l | l', m_l') \equiv \left\langle X_{l,mi}(1)\, X_{l',mi'}(2)\, \dfrac{e^2}{r^{12}}\, X_{l',mi}(1)\, X_{l,ml}(2) \right\rangle.$$

The larger the value of the exponent, the more contracted the d orbital, the more the Fe behaves as atomic Fe in its active site complex. However, we see that even for largest value of orbital exponent considered, 30, values of B and C are only 1/2 that of the experimentally determined B and C values for atomic Fe. In our IEHT calculations we have used a value of $\xi 3d = 2.72$ chosen to optimize Fe-
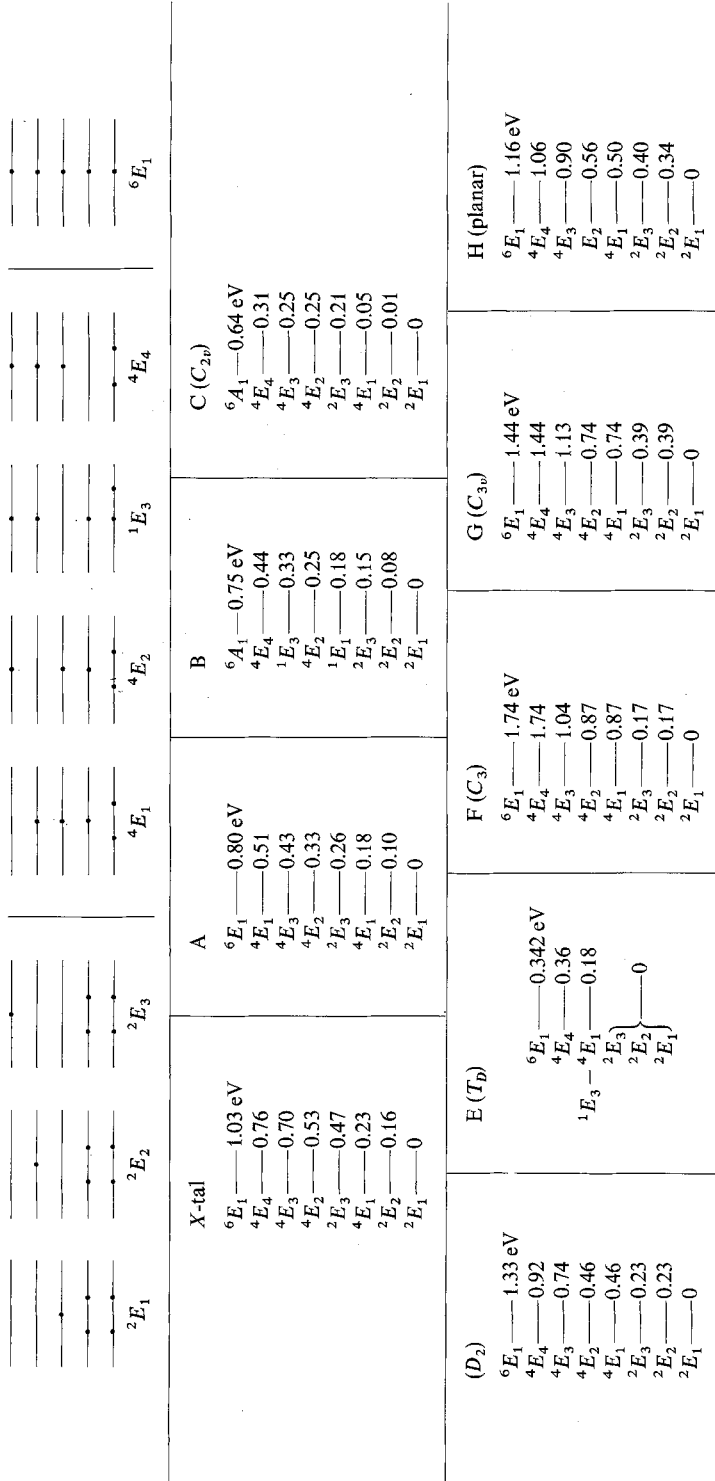
G. H. Loew *et al.*

X-tal

$^6E_1$ —— 1.03 eV
$^4E_4$ —— 0.76
$^4E_3$ —— 0.70
$^4E_2$ —— 0.53
$^2E_3$ —— 0.47
$^4E_1$ —— 0.23
$^2E_2$ —— 0.16
$^2E_1$ —— 0

A

$^6E_1$ —— 0.80 eV
$^4E_4$ —— 0.51
$^4E_3$ —— 0.43
$^4E_2$ —— 0.33
$^2E_3$ —— 0.26
$^4E_1$ —— 0.18
$^2E_2$ —— 0.10
$^2E_1$ —— 0

B

$^6A_1$ —— 0.75 eV
$^4E_4$ —— 0.44
$^1E_3$ —— 0.33
$^4E_2$ —— 0.25
$^1E_1$ —— 0.18
$^2E_3$ —— 0.15
$^2E_2$ —— 0.08
$^2E_1$ —— 0

C (C_{2v})

$^6A_1$ —— 0.64 eV
$^4E_4$ —— 0.31
$^4E_3$ —— 0.25
$^4E_2$ —— 0.25
$^2E_3$ —— 0.21
$^4E_1$ —— 0.05
$^2E_2$ —— 0.01
$^2E_1$ —— 0

(D_2)

$^6E_1$ —— 1.33 eV
$^4E_4$ —— 0.92
$^4E_3$ —— 0.74
$^4E_2$ —— 0.46
$^4E_1$ —— 0.46
$^2E_3$ —— 0.23
$^2E_2$ —— 0.23
$^2E_1$ —— 0

E (T_D)

$^6E_1$ —— 0.342 eV
$^4E_4$ —— 0.36
$^4E_1$ —— 0.18
$^1E_3$ — $^4E_1$
$^2E_3$
$^2E_2$ } 0
$^2E_1$

F (C_3)

$^6E_1$ —— 1.74 eV
$^4E_4$ —— 1.74
$^4E_3$ —— 1.04
$^4E_2$ —— 0.87
$^4E_1$ —— 0.87
$^2E_3$ —— 0.17
$^2E_2$ —— 0.17
$^2E_1$ —— 0

G (C_{3v})

$^6E_1$ —— 1.44 eV
$^4E_4$ —— 1.44
$^4E_3$ —— 1.13
$^4E_2$ —— 0.74
$^4E_1$ —— 0.74
$^2E_3$ —— 0.39
$^2E_2$ —— 0.39
$^2E_1$ —— 0

H (planar)

$^6E_1$ —— 1.16 eV
$^4E_4$ —— 1.06
$^4E_3$ —— 0.90
E_2 —— 0.56
$^4E_1$ —— 0.50
$^2E_3$ —— 0.40
$^2E_2$ —— 0.34
$^2E_1$ —— 0

Energy level columns: $^2E_1$ $^2E_2$ $^2E_3$ $^4E_1$ $^4E_2$ $^1E_3$ $^4E_4$ $^6E_1$

Fig. 4. Energies of 8 configurations calculated from IEHT relative to the lowest configuration energy $^2E_1$. a ^SE_i = configuration energy of ith configuration with (S − 1) half-filled MO's

Table 2. B, C^a corrections as a function of ξ_{Fe-3d}

ξ_{3d}^b	2.72	3.73	6.00	11.5	15	18	22	26	30
B	0.005 eV	0.0066	0.0106	0.0204	0.0266	0.0319	0.0390	0.0461	0.0532
C	0.019 eV	0.0236	0.0423	0.0811	0.1058	0.1269	0.1551	0.1833	0.2116

[a] 2-electron corrections in terms of Racah parameters B, C (Ref. [15]). Exp. value for Fe atom: B = 0.1 eV; C = 0.436 eV.
[b] $\xi 3d$ = Orbital exponent in radial part of Fe $3d$ function.

Table 3. Relative term energies (eV) at X-point^a for $^6A_1$ ground state

Sym.	O_1, O_2	A	B	$C_{(C_{2v})}$	$(D_{(D_2)})$	$E_{(T_D)}$	$F^d_{(C_3)}$	$G^d_{(C_{3v})}$	$H_{(C_{2h})}$
$\xi^c \int_{3d\text{-}Fe}$ X-point		18	16	23	none	7	9	6	9
$^0A_1^b$	0	0	0	0	0	0	0	0	0
$^4E_1$	0	0	0	0	-0.10	0	0	0	0
$^4E_2$	0.96	0.90 eV	0.84 eV	0.22	-0.10	$+0.07^e$	0.28	0.17	0.79
$^4E_3$	0.62	0.25	1.32	0.22	$+0.14$	$+0.31^e$	0.82	0.95	0.82
$^4E_4$	1.20	1.44	0.84	0.26	$+0.41$	$+0.39^e$	1.12	1.01	0.91
$^2E_1$	0.85	0.95	0.75	0.18	-0.35	$+0.08$	0.47	0	0.23
$^2E_2$	0.98	1.05	0.83	0.18	-0.58	$+0.08$	0.63	$+0.13$	0.56
$^2E_3$	1.02	1.21	0.90	0.38	$+0.58$	$+0.08$	0.78	0.28	0.71

[a] X-point of $^4E_1 - {}^6A_1$ energies, for smaller exchange corrections first $^2E_1$ then $^4E_1$ is ground state.
[b] Terms labelled by configuration from which they come.
[c] Value of ξ_{Fe-3d} at which $^6A_1$ becomes ground state. This quantity is a measure of magnitude of electron correlation correction needed to make $^6A_1$ c.s.
[d] In these symmetries, all quartet states chosen are doubly degenerate.
[e] Doubly degenerate value.

ligand overlap (9). We see that for this value of the exponent, B and C have only 5% of the free atom value.

In Table 2 is given the minimum value of the orbital exponent required to make the sextet state the ground state for each symmetry. The greater the ξ value required, the greater the electron correlation energy that was needed to overcome the difference in configuration energy. We see that the sextet state most easily becomes the ground state in T_D symmetry and never becomes the ground state in the D_2 version of tetrahedral symmetry (conformer D). Also given in this table is the relative energy of all the remaining quartet and doublet states at the cross point which have been calculated using Eqs. (1)–(3). For smaller exchange corrections first a doublet and then a quartet state is the ground state.

The energy intervals given in Table 3, represent the minimum calculated values of $d-d$, spin-forbidden electronic transition energies. An experimental determination of the lowest $^6A_1 \rightarrow {}^4E_1$ transition energy would tell us how far from the cross point ($\langle {}^6E_1 - {}^4E_1 \rangle = 0$) the sextet state in oxidized rubredoxin is. Lacking this information, we have systematically augmented this energy interval

in our spin-orbit calculations while keeping the relative energy ordering shown in Table 3 for all other energy intervals.

Having calculated the electron distribution and energies of the active site complex, we then used these to calculate a variety of specific properties of the oxidized rubredoxins as a function of conformation.

References

1. Lovenberg, W., Sobel, B. E.: Proc. Nat. Acad. Sci. USA **54**, 193 (1965)
2a. Herriott, J. R., Sieker, L. C., Jensen, L. H., Lovenberg, W.: J. Mol. Biol. **50**, 391 (1970)
2b. Jensen, L. H.: Latest X-ray results received 10/12/72 by private communication
2c. Jensen, L. H.: Results received 3/29/72 by private communication
3. Eaton, W. A., Lovenberg, W.: JACS **92**, **24**, 7195 (1970)
4. Eaton, W. A., Palmer, G., Fee, J. A., Kimura, T., Lovenberg, W.: Proc. Nat. Acad. Sci. USA **68**, no. 12, 3015 (1971)
5. Philipps, W. D., Poe, M., Weiher, J. F., MacDonald, C. C., Lovenberg, W.: Nature **227**, 547 (1970)
6. Peisach, J., Blumberg, W. D., Lode, E. T., Coon, M. J.: J. Biol. Chem. **246**, 5877 (1971)
7. Rao, K. K., Evans, M. C. W., Cammack, R., Hall, D. O., Thompson, C. L., Jackson, P. J., Johnson, C. E.: Biochem. J. **129**, 1063 (1972)
8. Zerner, M., Gouterman, M.: Theoret. Chim. Acta (Berl.) **4**, 44 (1966)
9. Zerner, M., Gouterman, M., Kobayashi, H.: Theoret. Chim. Acta (Berl.) **6**, 363 (1966)
10. Mulliken, R. S.: J. Chem. Physics **23**, 1833, 2338, 2343 (1955)
11. Clementi, E.: Tables of atomic orbital functions. IBM San Jose Research Laboratory Report
12. Zerner, M.: Ph. D. Thesis, Harvard University, Department of Chemistry 1966, private communication
13. Griffith, J. C.: The theory of transition metal ions, p. 63–105, 437. Cambridge University Press 1964
14. Alchemy program obtained from Drs. A. D. McLean, Bowen Liu, IBM San Jose Research Laboratories

Dr. G. H. Loew
Dept. of Genetics
Stanford University
Medical Center
Stanford, California 94305
USA